Letter

Bias-field digitized counterdiabatic quantum optimization

Alejandro Gomez Cadavid,[1,2] Archismita Dalal,[1] Anton Simen,[1,2] Enrique Solano,[1,*] and Narendra N. Hegade[1,†]
[1]*Kipu Quantum GmbH, Greifswalderstrasse 212, 10405 Berlin, Germany*
[2]*Department of Physical Chemistry, University of the Basque Country UPV/EHU, Apartado 644, 48080 Bilbao, Spain*

(Received 15 July 2024; accepted 27 February 2025; published 9 April 2025)

We introduce a method for solving combinatorial optimization problems on digital quantum computers, where we incorporate auxiliary counterdiabatic (CD) terms into the adiabatic Hamiltonian, while integrating bias terms derived from an iterative digitized counterdiabatic quantum algorithm. We call this protocol bias-field digitized counterdiabatic quantum optimization (BF-DCQO). Designed to effectively tackle large-scale combinatorial optimization problems, BF-DCQO demonstrates resilience against the limitations posed by the restricted coherence times of current quantum processors and shows clear enhancement even in the presence of noise. Additionally, our purely quantum approach eliminates the dependency on classical optimization required in hybrid classical-quantum schemes, thereby circumventing the trainability issues often associated with variational quantum algorithms. Through the analysis of an all-to-all connected general Ising spin-glass problem, we exhibit a polynomial scaling enhancement in ground-state success probability compared to traditional DCQO and finite-time adiabatic quantum optimization methods. Furthermore, it achieves scaling improvements in ground-state success probabilities, increasing by up to two orders of magnitude, and offers an average 1.3× better approximation ratio than the quantum approximate optimization algorithm for the problem sizes studied. We validate these findings through experimental implementations on both trapped-ion quantum computers and superconducting processors, tackling a maximum weighted independent set problem with 36 qubits and a spin glass on a heavy-hexagonal lattice with 100 qubits, respectively. These results mark a significant advancement in gate-based quantum computing, employing a fully quantum algorithmic approach.

DOI: 10.1103/PhysRevResearch.7.L022010

Introduction. Ising spin-glass problems are of utmost interest in both science and industry due to their vast applications. Particularly, combinatorial optimization problems, which can be formulated as solving for low-energy states of Ising spin-glass Hamiltonians, exemplify such applications [1]. Generally, these complex optimization problems belong to the NP-hard class, making them difficult to solve on classical computers. Recent theoretical and experimental developments in this area make it a crucial topic for further exploration on current quantum computers [2–4]. A major drawback of current quantum computing hardware is its limited coherence time, connectivity, and presence of noise. These limitations pose significant challenges for widely studied quantum optimization algorithms such as the adiabatic quantum optimization (AQO) algorithm and the quantum approximate optimization algorithm (QAOA) [5,6]. To overcome these challenges, several alternative methods have been proposed, including the counterdiabatic (CD) protocols. In the case of AQO, CD protocols help to speed up the evolution and reduce the quantum circuit depth by suppressing nonadiabatic transitions through the addition of CD terms [7–9]. For QAOA, CD protocols aid in designing an efficient variational circuit ansatz that quickly converges towards the solution [10,11]. Despite the advantages of CD protocols, tackling large-scale problems remains a challenge, especially when it is crucial to consider higher-order CD terms, which increases the number of quantum gates.

In this Letter, we propose a method to tackle general Ising spin-glass instances with long-range interactions through an iterative algorithm. The output from each iteration is fed back as a bias to the input of the next iteration. This combined approach of a digitized counterdiabatic quantum optimization algorithm with a bias field, called BF-DCQO, shows a drastic reduction in the time to reach both exact and approximate solutions compared to state-of-the-art approaches. This includes DCQO [12] as well as hybrid variational quantum algorithms such as QAOA, which have been recently applied to large-scale problems [13–15]. Additionally, BF-DCQO does not require any classical optimization subroutines, thus overcoming the trainability issues faced by variational quantum optimization algorithms [16]. We experimentally demonstrate the potential of the proposed method on trapped-ion quantum computers with up to fully connected 36 qubits and superconducting quantum processors with sparsely connected 100 qubits. We will discuss the advantages of the proposed BF-DCQO method in the light of competing protocols for approaching quantum advantage for industry use cases.

*Contact author: enr.solano@gmail.com
†Contact author: narendrahegade5@gmail.com

DCQO algorithm. An adiabatic quantum optimization protocol to find the ground state of an Ising spin-glass problem with all-to-all connectivity is described by the Hamiltonian $H_{\rm ad}(\lambda) = [1-\lambda(t)]H_i + \lambda(t)H_f$. Here, H_i is the initial Hamiltonian whose ground state can be easily prepared, typically chosen as a transverse field $H_i = -\sum_{i=1}^{N}\sigma_i^x$ with the ground state $|+\rangle^{\otimes N}$, where N is the number of spins. The final Hamiltonian, corresponding to the spin glass, is $H_f = \sum_{i<j}^{N} J_{ij}\sigma_i^z\sigma_j^z + \sum_{i=1}^{N} h_i\sigma_i^z$. Here, λ is a time-dependent control function that describes the adiabatic path. In the adiabatic limit, i.e., $\dot{\lambda}(t) \to 0$, the system follows the instantaneous eigenstates. However, in practice, following the slow adiabatic evolution is affected by hardware noise and the limited coherence time. On the other hand, fast evolution results in nonadiabatic transitions. To overcome this challenge, CD protocols have been proposed [7,8]. In CD protocols, the idea is to introduce an auxiliary velocity-dependent $[\dot{\lambda}(t)]$ term to the Hamiltonian to suppress nonadiabatic transitions. This takes the form $H_{\rm cd}(\lambda) = H_{\rm ad}(\lambda) + \dot{\lambda}A_\lambda$, where A_λ is known as the adiabatic gauge potential [17]. Obtaining and realizing A_λ is a highly resource-demanding task for many-body Hamiltonians. Rather, there are several proposals to obtain this in an approximate way [18–23]. We consider the nested commutator method where the adiabatic gauge potential can be written as the series expansion $A_\lambda^{(l)} = i\sum_{k=1}^{l}\alpha_k(t)O_{2k-1}(t)$. Here, l is the expansion order, and the operator $O_k(t) = [H_{\rm ad}, O_{k-1}(t)]$ with $O_0(t) = \partial_\lambda H_{\rm ad}$. In the limit $l \to \infty$, the exact A_λ can be obtained. The CD coefficient $\alpha_k(t)$ can be calculated by variational minimization as detailed in the Supplemental Material [24]. To solve for the Ising spin-glass problem, we simply consider the first-order approximation as $A_\lambda^{(1)} = -2\alpha_1[\sum_{i=1}^{N} h_i\sigma_i^y + \sum_{i<j}^{N} J_{ij}(\sigma_i^y\sigma_j^z + \sigma_i^z\sigma_j^y)]$. The time evolution of the Hamiltonian in the given equation, even with the first-order CD term, is a challenging task on current analog quantum processors due to a lack of flexibility. Also, an important fact to notice is that the obtained CD terms are nonstoquastic with off-diagonal matrix entries being imaginary. The realization of such terms on current quantum annealers is unfeasible. To overcome this challenge, digitized counterdiabatic quantum protocols have been proposed to realize the CD protocols on gate-model quantum computers [25]. Not only does the digital approach provide the flexibility to realize arbitrary CD terms, it also helps to further improve the CD protocols because of the flexibility in the control parameters. To realize the time evolution of the CD Hamiltonian, we use the first-order product formula [26] with a number of Trotter steps $n_{\rm trot}$, step size Δt, and total evolution time T. The unitary describing the evolution is given by $|\psi(T)\rangle = [\prod_{k=1}^{n_{\rm trot}}\prod_{j=1}^{n_{\rm terms}}\exp\{-i\Delta t\gamma_j(k\Delta t)H_j\}]|\psi_i\rangle$. Here, $|\psi_i\rangle$ is the initial ground state and $H_{\rm cd} = \sum_{j=1}^{n_{\rm terms}}\gamma_j(t)H_j$, where $n_{\rm terms}$ is the number of local Pauli operators H_j. Each product of matrix exponentials is decomposed into quantum gates with one- and two-qubit gates. Even with the first-order CD approximation, a polynomial scaling enhancement in ground-state success probability has been shown in comparisons to finite-time AQO [12,27]. Going for higher-order CD terms can improve the results further but this comes at the cost of additional quantum gates. The main advantage of this approximate CD protocol is that, even with a very short evolution time or circuit depth, one can obtain low-energy states in comparison to digitized adiabatic evolution. To obtain similar performance, one would require very long-depth digitized adiabatic evolution, which is not feasible because of the limited coherence time and the noise. This main feature is the key to developing the concept of bias field for the CD protocol.

DCQO with longitudinal bias field. Initialization plays a crucial role in the success of AQO and DCQO. Instead of starting with a random initial state, beginning with a good one that encodes some information about the final solution is beneficial [28,29]. Several proposals exist for such warm starting techniques, wherein inexpensive classical methods are used to solve a relaxed version of the problem and then utilize this solution as an input for the quantum algorithm [30,31]. These techniques inherit the performance guarantee of the classical algorithm. Then, we propose a different approach where the solution from DCQO is fed back as a bias to the input state for the next iteration. The total Hamiltonian, which includes the longitudinal bias field, is defined as

$$H(\lambda) = [1-\lambda(t)]\tilde{H}_i + \lambda(t)H_f + \dot{\lambda}A_\lambda^{(l)}, \tag{1}$$

with $\tilde{H}_i = \sum_{i=1}^{N}[h_i^x\sigma_i^x - h_i^b\sigma_i^z]$. Here, the value of the longitudinal bias field, $h_i^b = \langle\sigma_i^z\rangle$, is obtained by measuring the qubits in the computational basis in each iteration. Note that we start from DCQO, which is equivalent to setting all bias fields to zero. Since DCQO is expected to sample low-energy states of the spin-glass Hamiltonian, the Pauli-Z expectation value can serve as an effective bias for the next iteration, steering the dynamics toward the actual solution. Because the bias term alters the initial Hamiltonian and, consequently, the initial ground state, the new ground state $|\tilde{\psi}_i\rangle$ must be used as the input for the next iteration. The smallest eigenvalue of the single-body operator $[h_i^x\sigma_i^x - h_i^b\sigma_i^z]$ is given by $\lambda_i^{\rm min} = -\sqrt{(h_i^b)^2+(h_i^x)^2}$, and its associated eigenvector is $|\tilde{\phi}\rangle_i = R_y(\theta_i)|0\rangle_i$, where $\theta_i = 2\tan^{-1}(\frac{h_i^b+\lambda_{\rm min}}{h_i^x})$. Therefore, the ground state of $\tilde{H}_i$ can be prepared using N y-axis rotations as $|\tilde{\psi}_i\rangle = \bigotimes_{i=1}^{N}|\tilde{\phi}\rangle_i = \bigotimes_{i=1}^{N}R_y(\theta_i)|0\rangle_i$. In Fig. 1(a), the schematic diagram depicting the BF-DCQO is shown.

To analyze the performance of the BF-DCQO, we consider 400 random instances of the spin-glass problem, with coupling J_{ij} and h_i obtained from a Gaussian distribution with a mean of 0 and a variance of 1. The scheduling function is $\lambda(t) = \sin^2[\frac{\pi}{2}\sin^2(\frac{\pi t}{2T})]$ and we use $h_i^x = -1$. We only consider first-order CD terms and the CD coefficient changes during each iteration since the initial Hamiltonian changes. In this case, we analytically calculate the exact form of the CD coefficient α_1 for the Hamiltonian in Eq. (1). Figure 1(b) illustrates the ground-state success probability with increasing system size for BF-DCQO with ten iterations and naive DCQO, given a fixed evolution time T with three Trotter steps. In both cases, the success probability $p_{\rm gs} = |\langle\psi_{\rm gs} \mid \psi_f(T)\rangle|^2$, where $|\psi_{\rm gs}\rangle$ is the actual ground state of the spin-glass Hamiltonian, decreases exponentially with system size. However, the exponential factor for BF-DCQO is smaller than that for DCQO, indicating a polynomial scaling advantage. We noticed that not all 400 instances are improved by the inclusion of the bias field. In some cases, if the solution from the first iteration of DCQO leads to undesired outcomes, employing an

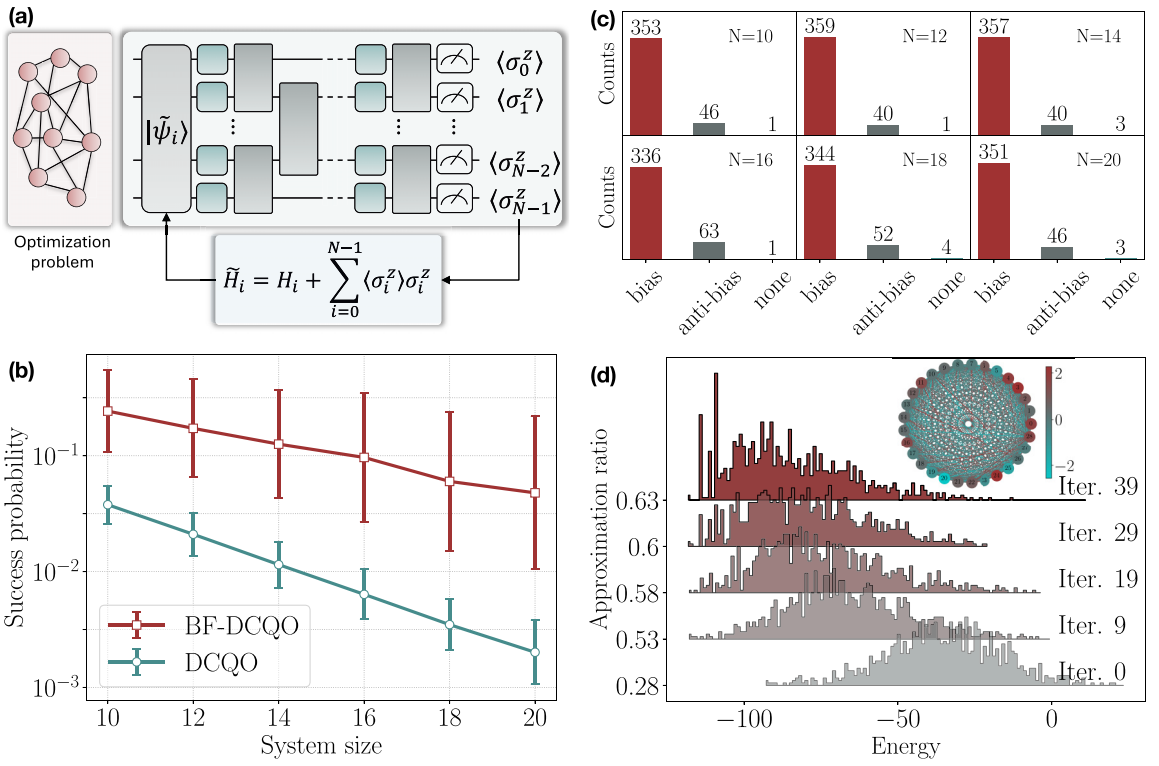

FIG. 1. BF-DCQO for the Ising spin-glass problem with an all-to-all interaction. In (a), the schematic of the BF-DCQO procedure is shown. In (b), the ground-state success probability is plotted for system sizes ranging from 10 to 20 qubits. For each system size, 400 randomly generated spin-glass instances are taken from a normal distribution with a mean of 0 and a variance of 1. We present the scaling of the BF-DCQO algorithm with ten iterations and the standard DCQO, with simulation parameters $\Delta t = 0.1$ and $n_{\text{trot}} = 3$. The error bars represent the standard deviation of the random instances. In (c), the classification of the 400 instances using enhancement in success probability as a criterion, counting the number of instances successfully tackled by either the bias- or antibias-field DCQO, and those that failed in both cases. In (d), emulation results for a randomly generated spin-glass problem with 29 qubits are shown. We performed 39 iterations of BF-DCQO, displaying the increasing approximation ratio on the y axis. For each iteration, we used $n_{\text{trot}} = 2$, $n_{\text{shots}} = 1000$, and the IonQ Forte 1 noise model, accessed through IonQ Cloud [32]. Additionally, the associated all-to-all connected graph is depicted.

antibias field $h_i^b = -\langle\sigma_i^z\rangle$ may help suppress these outcomes. In Fig. 1(c), the number of instances enhanced by the bias field is depicted. For the unsuccessful instances, employing an antibias field shows improvement. However, there are few instances where both the bias and antibias fields fail. This is primarily due to the simulation parameters we have chosen in this work, and altering them may lead to successful results.

To evaluate the performance of the algorithm in the presence of hardware noise, we use a noisy emulator that mimics the actual noise model of a trapped-ion hardware system, IonQ Forte. We consider a fully connected 29-qubit spin-glass instance and implement the BF-DCQO algorithm. The energy distribution across each iteration is shown in Fig. 1(d). Remarkably, even with just $n_{\text{trot}} = 2$ steps and the number of shots $n_{\text{shots}} = 1000$, the algorithm guides the dynamics toward the solution. By iteration 29, the exact ground state was obtained. Additionally, it is clear that the approximation ratio $E_{\text{obtained}}/E_{\text{gs}}$ improves with each iteration.

An important aspect of BF-DCQO is that it does not require any classical optimization subroutines as in variational quantum algorithms (VQAs). This feature makes it an impressive approach, as the main drawback of VQA lies in trainability issues such as barren plateaus and local minima. The presence of noise makes it even harder to rely on VQAs. Since we have already seen the successful performance of BF-DCQO in noisy conditions, we compare its performance with QAOA, a widely used variational quantum optimization algorithm. We consider ten random instances of the long-range spin-glass problem across various sizes. Ground-state success probability and approximation ratio are used as metrics for comparison. We also compare BF-DCQO with bias-field QAOA in the Supplemental Material [24].

To maintain the same circuit depth, we consider QAOA with $p = 3$ layers and BF-DCQO with $n_{\text{trot}} = 3$. For optimizing the QAOA circuit, we use the COBYLA optimizer with a maximum of 300 iterations. For each instance, the best solution out of 20 random initializations is considered for QAOA. A similar performance is obtained by doing quantum-annealing initialization, as in Ref. [33]. For BF-DCQO, we employ just ten iterations of feedback. In Fig. 2, we plot the success probability enhancement ratio, which is the ratio of the ground-state success probability obtained with BF-DCQO vs QAOA, as well as the enhancement ratio of the approximation ratio. Despite requiring two orders of magnitude fewer iterations, BF-DCQO outperforms QAOA in both metrics. Moreover, the success probability enhancement ratio increases with system size, showing a 75× improvement for

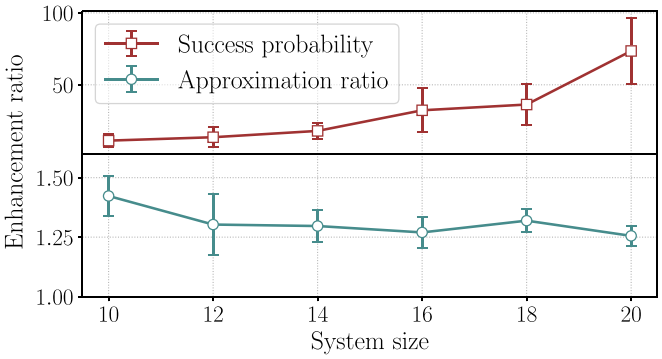

FIG. 2. Comparison between simulated BF-DCQO and QAOA ($p = 3$). The analysis was conducted on ten different random all-to-all connected spin-glass instances, with system sizes ranging from 10 to 20 qubits. For QAOA, we used 20 different random initializations with the COBYLA optimizer and kept the best, setting the maximum number of iterations at 300. This was contrasted with ten iterations of BF-DCQO, where $n_{\text{trot}} = 3$.

the 20-qubit case. On average, we observe a 1.3× improvement in the approximation ratio with BF-DCQO.

Experimental implementation. For the experimental validation of BF-DCQO, we consider a 36-qubit trapped-ion quantum processor, IonQ Forte, and a 127-qubit superconducting quantum processor, *ibm_brisbane*. We explore two problems that can be suitably mapped to the hardware connectivity: a randomly generated weighted maximum independent set (WMIS) problem with 36 nodes, implemented on trapped-ion hardware, and an instance of the Ising spin-glass problem on a heavy-hexagonal lattice with 100 spins, implemented on superconducting hardware.

The WMIS is a combinatorial optimization problem where the objective is to identify a subset of vertices in a graph that are mutually nonadjacent (an independent set) and have the highest possible total weight. Given a graph $G = (V, E)$ with vertices V and edges E, each vertex $v \in V$ has an associated weight $w(v)$. The task is to find a subset of vertices $I \subseteq V$ such that no two vertices in I are connected by an edge in E, while maximizing the sum of the weights of the selected vertices,

$$\text{Maximize} \quad \sum_{v \in I} w(v), \quad \text{subject to} \quad (u, v) \notin E \quad \forall\, u, v \in I.$$

This problem is NP-hard because it generalizes the classic MIS problem by incorporating vertex weights. The WMIS problem can be mapped to the Ising spin-glass Hamiltonian by associating a binary spin variable with each vertex, and defining interactions that penalize adjacent vertices that are both included, while rewarding vertices that are selected based on their weights. Since in the WMIS problem the interactions between the qubits can be long range, trapped-ion systems are well suited to tackle this problem without requiring any SWAP gates. In Fig. 3(a), the experimental result from IonQ Forte for a 36-node WMIS is shown. To optimize access to the hardware, we first ran the BF-DCQO on an ideal local simulator and then ran only the final circuit corresponding to the last iteration on the hardware. The error-mitigated experimental result is in close agreement with the ideal simulation result. In the experiment, we considered $n_{\text{trot}} = 3$, $n_{\text{shots}} = 2500$, and used hardware native gates for circuit implementation. Additionally, we performed debias error mitigation [34] and circuit optimization to reduce the total gate counts further. For the considered WMIS problem, the maximum independent set size is 16, and the obtained independent set size from the experiment is 11.

As a second example, we consider a spin-glass problem on a heavy-hexagonal lattice. Since the interaction terms in the problem Hamiltonian match the hardware connectivity, we can consider a large system size of 100 qubits on the *ibm_brisbane* hardware. In Fig. 3(b), we show the ideal simulation results for DCQO and BF-DCQO, and the experimental result for BF-DCQO. We also consider a classical solver, GUROBI [36], as a reference. We notice that, even with just ten iterations, BF-DCQO provides a drastic enhancement compared to DCQO. Additionally, in the absence of noise, BF-DCQO reaches the solution obtained from GUROBI with just two Trotter steps. Although the experimental results are slightly different from the ideal result due to noise, the performance is better than the ideal DCQO. More details on the

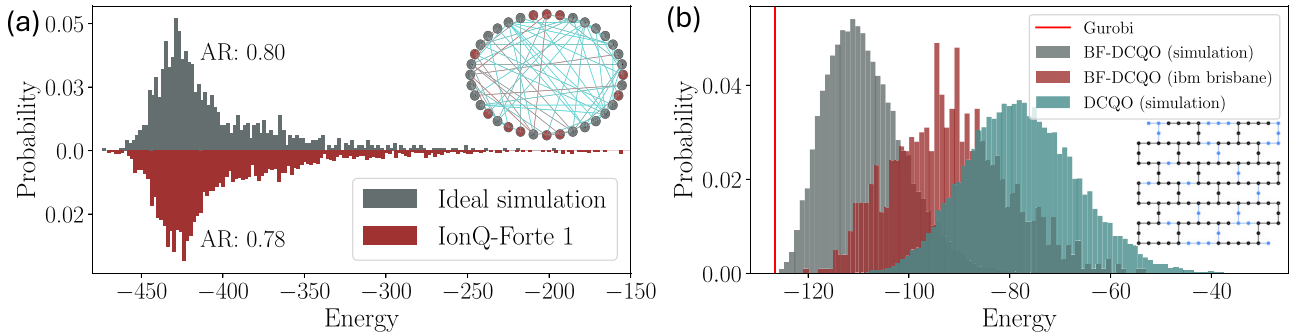

FIG. 3. Experimental results: In (a), the ninth iteration of BF-DCQO for a randomly generated 36-node weighted MIS instance is shown. For the simulations, we used $n_{\text{trot}} = 3$, and $n_{\text{shots}} = 1000$. In the experimental case on IonQ Forte 1, only the ninth iteration was run, using $n_{\text{shots}} = 2500$ with error mitigation. The MIS size was 16, and we obtained an independent set of size 11, as depicted in the graph. In (b), the eighth iteration of BF-DCQO for a nearest-neighbor randomly generated 100-qubit spin-glass instance is displayed. For these simulations, we used $n_{\text{trot}} = 2$ and $n_{\text{shots}} = 25000$ and the QISKIT AER MPS simulator [35]. For the experimental results on *ibm_brisbane*, $n_{\text{shots}} = 1000$ was used. Additionally, the circuit layout on the hardware is shown.

experimental implementation can be found in the Supplemental Material [24].

Discussion and conclusion. We introduced BF-DCQO, an iterative nonvariational quantum optimization algorithm designed to tackle combinatorial optimization problems mapped to long-range Ising spin-glass problems. By feeding back the solution from each iteration as the input for the next one, BF-DCQO incrementally refines the initial ground state, bringing it progressively closer to the final ground state. This iterative approach, combined with CD protocols that prepare low-energy states using short-depth quantum circuits, makes BF-DCQO well suited for large-scale combinatorial optimization problems on current quantum hardware with limited coherence times.

Our simulation results demonstrate a polynomial scaling advantage in ground-state success probability compared to finite-time digitized AQO and DCQO for fully connected spin-glass problems. Additionally, noisy simulations with realistic noise models for a fully connected 29-qubit spin-glass problem showcase the algorithm's robustness, achieving exact ground states despite the presence of noise. The absence of classical optimization subroutines in BF-DCQO helps mitigate trainability issues commonly associated with VQAs. Comparisons with the QAOA reveal significant enhancements in ground-state success probability and approximation ratios while requiring fewer computational resources. Although BF-DCQO shows great promise, as a purely quantum algorithm, future work could also explore hybrid versions incorporating variational parameters and higher-order CD terms. Experimental validation on a 36-qubit trapped-ion quantum computer and a 100-qubit superconducting quantum computer confirmed good agreement with ideal simulations. Looking ahead, BF-DCQO could tackle more challenging instances of long-range spin-glass problems on next-generation trapped-ion hardware with over 60 qubits, potentially providing empirical evidence of quantum speedup by comparing its performance with classical algorithms.

[1] A. Lucas, Ising formulations of many NP problems, Front. Phys. **2**, 74887 (2014).

[2] N. Pirnay, V. Ulitzsch, F. Wilde, J. Eisert, and J.-P. Seifert, An in-principle super-polynomial quantum advantage for approximating combinatorial optimization problems via computational learning theory, Sci. Adv. **10**, eadj5170 (2024).

[3] S. Boulebnane and A. Montanaro, Solving boolean satisfiability problems with the quantum approximate optimization algorithm, PRX Quantum **5**, 030348 (2024).

[4] S. Ebadi, A. Keesling, M. Cain, T. T. Wang, H. Levine, D. Bluvstein, G. Semeghini, A. Omran, J.-G. Liu, R. Samajdar *et al.*, Quantum optimization of maximum independent set using Rydberg atom arrays, Science **376**, 1209 (2022).

[5] T. Albash and D. A. Lidar, Adiabatic quantum computation, Rev. Mod. Phys. **90**, 015002 (2018).

[6] E. Farhi, J. Goldstone, and S. Gutmann, A quantum approximate optimization algorithm, arXiv:1411.4028.

[7] M. Demirplak and S. A. Rice, Adiabatic population transfer with control fields, J. Phys. Chem. A **107**, 9937 (2003).

[8] M. V. Berry, Transitionless quantum driving, J. Phys. A: Math. Theor. **42**, 365303 (2009).

[9] A. del Campo, Shortcuts to adiabaticity by counterdiabatic driving, Phys. Rev. Lett. **111**, 100502 (2013).

[10] P. Chandarana, N. N. Hegade, K. Paul, F. Albarrán-Arriagada, E. Solano, A. del Campo, and X. Chen, Digitized-counterdiabatic quantum approximate optimization algorithm, Phys. Rev. Res. **4**, 013141 (2022).

[11] P. Chandarana, N. N. Hegade, I. Montalban, E. Solano, and X. Chen, Digitized counterdiabatic quantum algorithm for protein folding, Phys. Rev. Appl. **20**, 014024 (2023).

[12] N. N. Hegade, X. Chen, and E. Solano, Digitized counterdiabatic quantum optimization, Phys. Rev. Res. **4**, L042030 (2022).

[13] E. Pelofske, A. Bärtschi, and S. Eidenbenz, Quantum annealing vs. QAOA: 127 qubit higher-order Ising problems on NISQ computers, in *High Performance Computing*, edited by A. Bhatele, J. Hammond, M. Baboulin, and C. Kruse (Springer Nature, Cham, 2023), pp. 240–258.

[14] E. Pelofske, A. Bärtschi, and S. Eidenbenz, Short-depth QAOA circuits and quantum annealing on higher-order Ising models, npj Quantum Inf. **10**, 30 (2024).

[15] N. Sachdeva, G. S. Hartnett, S. Maity, S. Marsh, Y. Wang, A. Winick, R. Dougherty, D. Canuto, Y. Q. Chong, M. Hush, P. S. Mundada, C. D. B. Bentley, M. J. Biercuk, and Y. Baum, Quantum optimization using a 127-qubit gate-model IBM quantum computer can outperform quantum annealers for nontrivial binary optimization problems, arXiv:2406.01743.

[16] S. Wang, E. Fontana, M. Cerezo, K. Sharma, A. Sone, L. Cincio, and P. J. Coles, Noise-induced barren plateaus in variational quantum algorithms, Nat. Commun. **12**, 6961 (2021).

[17] M. Kolodrubetz, D. Sels, P. Mehta, and A. Polkovnikov, Geometry and non-adiabatic response in quantum and classical systems, Phys. Rep. **697**, 1 (2017).

[18] D. Sels and A. Polkovnikov, Minimizing irreversible losses in quantum systems by local counterdiabatic driving, Proc. Natl. Acad. Sci. USA **114**, E3909 (2017).

[19] P. W. Claeys, M. Pandey, D. Sels, and A. Polkovnikov, Floquet-engineering counterdiabatic protocols in quantum many-body systems, Phys. Rev. Lett. **123**, 090602 (2019).

[20] T. Hatomura and K. Takahashi, Controlling and exploring quantum systems by algebraic expression of adiabatic gauge potential, Phys. Rev. A **103**, 012220 (2021).

[21] Q. Xie, K. Seki, and S. Yunoki, Variational counterdiabatic driving of the Hubbard model for ground-state preparation, Phys. Rev. B **106**, 155153 (2022).

[22] K. Takahashi and A. del Campo, Shortcuts to adiabaticity in Krylov space, Phys. Rev. X **14**, 011032 (2024).

[23] C. Mc Keever and M. Lubasch, Towards adiabatic quantum computing using compressed quantum circuits, PRX Quantum **5**, 020362 (2024).

[24] See Supplemental Material at http://link.aps.org/supplemental/10.1103/PhysRevResearch.7.L022010 for the analytical calculation of the CD coefficient, details about the simulation and

experimental procedures, and additional results to support the concepts discussed in the main article.

[25] N. N. Hegade, K. Paul, Y. Ding, M. Sanz, F. Albarrán-Arriagada, E. Solano, and X. Chen, Shortcuts to adiabaticity in digitized adiabatic quantum computing, Phys. Rev. Appl. **15**, 024038 (2021).

[26] R. Barends, A. Shabani, L. Lamata, J. Kelly, A. Mezzacapo, U. Las Heras, R. Babbush, A. G. Fowler, B. Campbell, Y. Chen *et al.*, Digitized adiabatic quantum computing with a superconducting circuit, Nature (London) **534**, 222 (2016).

[27] A. Hartmann, G. B. Mbeng, and W. Lechner, Polynomial scaling enhancement in the ground-state preparation of Ising spin models via counterdiabatic driving, Phys. Rev. A **105**, 022614 (2022).

[28] T. Graß, Quantum annealing with longitudinal bias fields, Phys. Rev. Lett. **123**, 120501 (2019).

[29] T. Grass, Quantum annealing sampling with a bias field, Phys. Rev. Appl. **18**, 044036 (2022).

[30] D. J. Egger, J. Mareček, and S. Woerner, Warm-starting quantum optimization, Quantum **5**, 479 (2021).

[31] F. Truger, J. Barzen, M. Bechtold, M. Beisel, F. Leymann, A. Mandl, and V. Yussupov, Warm-starting and quantum computing: A systematic mapping study, ACM Comput. Surv. **56**, 229 (2023).

[32] IonQ, IonQ Quantum Cloud documentation, https://docs.ionq.com/.

[33] S. H. Sack and M. Serbyn, Quantum annealing initialization of the quantum approximate optimization algorithm, Quantum **5**, 491 (2021).

[34] A. Maksymov, J. Nguyen, Y. Nam, and I. Markov, Enhancing quantum computer performance via symmetrization, arXiv:2301.07233.

[35] Qiskit contributors, Qiskit: An open-source framework for quantum computing, https://doi.org/10.5281/zenodo.2573505.

[36] Gurobi Optimization, LLC, Gurobi Optimizer Reference Manual, https://www.gurobi.com.